Compact MIMO Microstrip Antenna for Wireless PAN

Shilpa Nandedkar[1*] and Shankar Nawale[2]
[1] Maharashtra Institute of Technology, Aurangabad, (MS), India
[2] N. B. Navale Sinhgad College of Engineering, Solapur, (MS), India
Email: shankarnawale125@gmail.com

***Abstract*—This article presents compact wideband four elements Many-Input Many-Output (MIMO) antenna using Defect Ground Structure (DGS). The proposed structure is dedicated to cover 4G-LTE/Sub 6 GHz bands in the 2.5/3.5/5.5 GHz frequency range and WLAN, Wi-Fi, and (LTE bands 41, 42, 43, 46, and 48). It also includes new radio (NR) technology which has different bands for 5G and (sub-6 GHz bands 47, 48). The designed antenna is very compact in size having dimensions of 28 mm × 29.58 mm × 0.8 mm. Isolation is achieved with square ring resonators (SRR). Isolation is further enhanced by inserting slots and SRRs between antennas. MIMO antenna characteristics such as high isolation (45 dB), low envelope correlation coefficient (0.01), and high diversity gain (10 dB) are measured. Furthermore, a wide impedance bandwidth of 8 GHz is measured. MIMO antenna is verified with a Software-Defined Radio (SDR) platform.**

***Index Terms*—Many-Input Many-Output (MIMO) antenna, isolation, Envelope Correlation Coefficient (ECC), square ring resonator**

I. Introduction

Many-Input Many-Output (MIMO) wireless communication systems use multiple antennas at the transmitter and/or the receiver to increase the transmission rate and the strength of the received signal. MIMO offers high gain, superior data rates, range, and reliability without requiring additional bandwidth or transmits power [1]. Multiple antennas with multiband having broader bandwidth are needed for the next-generation wireless communication systems. For making MIMO antenna compact in size, elements are placed close to each other, due to which coupling increases and it becomes an implementation issue in portable devices. For addressing such issues mm-wave-based MIMO architectures and antenna systems has been forecasted in recent literature to operate within the 5G and sub 6G bands [2]-[10]. Several decoupling techniques such as increasing spacing between elements, use of meta-material [2], parasitic structures with low index metamaterial [3], neutralization line [4], decoupling circuits [5], reflectors [6], defected ground structure [7], un-protruded multi-slot (UPMS) [8], triangular stub [9], chain shaped parasitic element [10], pattern diversity [11], a planar printed antenna on both side of substrate gives omnidirectional pattern diversity [12], reconfigurable MIMO antenna has been reported in many applications [13]-[17]. Each method has its own merits and demerits. Depending on the application, suitable techniques are preferred. Wireless personal area network (PAN) application requires more bandwidth within a limited range. Therefore, proposed structure is designed to get wider bandwidth.

Many compact MIMO antennas, having multiband, use band notch characteristics for separating bands or for reducing interference between them [18], [19]. For improving isolation between ports, electromagnetic band gap fractal MTM-EMBG [20] and metallic separation strips [21] are used. Wide impedance bandwidth is achieved with Dielectric Resonator Antenna (DRA) as reported in [22]-[24]. DRAs can be suitable candidates in comparison to conventional metallic antennas due to the increase in the frequency in modern wireless communication [25], but it has disadvantages of complexity and cost.

The requirement of an antenna in the wireless application includes low profile, low volume, lightweight, and low cost while maintaining good electrical properties such as return loss and isolation (10 dB). Space available for the antenna is shrinking all the time due to the requirement of all wireless devices. Wireless PAN and its applications are more encouraging on account of its benefits, for example, high information rate and little inclusion region. Gadgets working with Wi-Fi are laptops, tablets, wireless access points, cell phones, USB dongles, printers, shrewd watches, individual advanced aids, and so forth. Interconnection of these gadgets may incorporate individual PAN, Bluetooth, Ethernet, etc.

For wireless communication compact size printed monopole antennas are preferred due to its advantages of easy fabrication, omnidirectional radiation, and wide operation bandwidth [26]. Therefore, in the proposed structure a printed monopole was designed. The antenna was simulated by using CST microwave studio software.

The paper is organized as follows. Section II gives the design and stepwise modification of a single element. Section III shows the MIMO antenna and its parameters. It also indicates stepwise modification in the ground plane for isolation enhancement, comparison of experimental results with simulated results, and testing of MIMO antenna with Software Define Radio (SDR). Finally, the paper is concluded in Section IV.

Manuscript received September 27, 2022; revised November 13, 2022; accepted November 22, 2022.
*Corresponding author: Shilpa Nandedkar (email: Shilpa.nandedkar @mit.asia).

II. Experiment and Result

The following sub-section illustrates the design steps and their simulated parameters such as return loss, Voltage Standing Wave Ratio (VSWR), directivity, bandwidth, and radiation pattern.

A. Antenna Structure

Fig. 1 shows the geometry of the proposed single monopole antenna with optimized dimensions. It consists of a front view and a back view for Antenna 1 and Antenna 2. Antenna is designed and simulated in two steps.

Step I: For making the antenna cost effective, the substrate material of FR-4 is used. It has a specification as dielectric constant of 4.3, a thickness of 0.8 mm, and a loss tangent of 0.025. Ground and patch are made with conducting material of copper having a thickness of 0.1 mm. The frequency of operation is taken from 2 GHz to 9.78 GHz, since resonating frequency f_r is 5.89 GHz for Long Term Evolution (LTE) 47 band. Calculated dimensions of the monopole are of length 10 mm and width 1.43 mm.

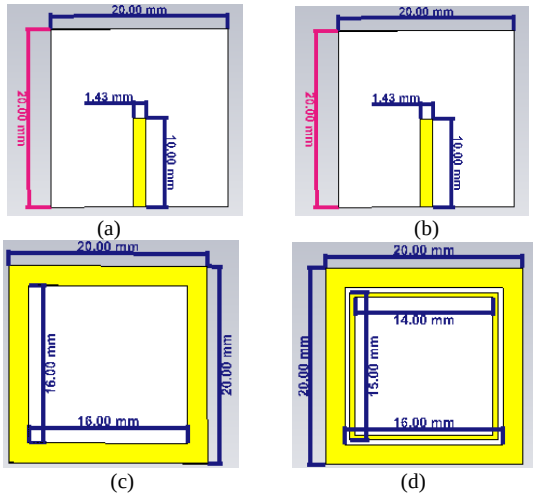

Fig. 1. Design steps of the proposed single antenna: (a) front view and (b) back view of Antenna 1, and (c) front view and (d) back view of Antenna 2.

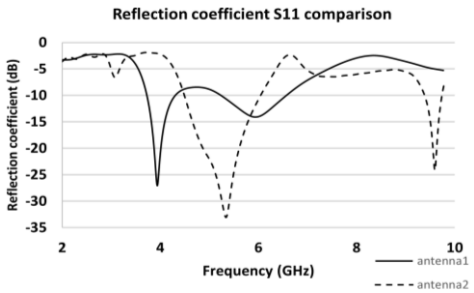

Fig. 2. Reflection coefficient curve for Antenna 1 and Antenna 2.

Fig. 2 shows frequency verses reflection coefficient S11 curve for Antenna 1 and Antenna 2. Simulation result shows that Antenna 1 has two frequency bands: 3.72 GHz to 4.26 GHz and 5.23 GHz to 6.56 GHz. It has a bandwidth of 574.4 MHz and an impedance bandwidth of 3.61 GHz. Furthermore, Antenna 2 is designed with modification in step-II.

Step-II: A square ring resonator (SRR) is added in ground for Antenna 2. SRR is designed using the following equation [6].

$$f = \frac{1}{2\pi}\sqrt{\frac{1}{L_T C_{eq}}} \quad (1)$$

Equation (1) gives frequency for resonator where L_T is equivalent inductance and C_{eq} is equivalent capacitance. Dimensions of SRR are 15 mm × 15 mm and width of 0.5 mm.

With Antenna 2, two frequency bands: 4.33 GHz to 6.29 GHz and 9.12 GHz to 10.00 GHz are obtained with bandwidths of 1.15 GHz and 0.347 GHz, respectively. Obviously, Antenna 2 has bigger bandwidth compared to Antenna 1.

In Table I, the directivity and VSWR are compared for these antennas which demonstrates that Antenna 2 exhibits better directivity, improved bandwidth (10 dB) for Band 1, and a good VSWR value as compared to Antenna 1. It also shows return loss (S11) for both bands which indicates Antenna 2 is having a better performance; therefore, it is preferred for the MIMO antenna.

Table I: Comparison of Antenna Structures

Antenna	Band 1 (GHz)		Band 2 (GHz)		Directivity	VSWR
	S11 (dB)	VSWR (2:1)	S11 (dB)	VSWR (2:1)		
Antenna 1	-27.03	3.72-4.29	-14.08	5.23-6.56	3.69	1.09
Antenna 2	-33.06	4.49-6.04	-24.12	9.38-9.73	4.27	1.04

B. MIMO Structure

To extend design steps as explained in earlier subsection, MIMO antennas are designed in which four monopoles are placed with four ports. The ground structure is modified in further steps for enhancing isolation. Theoretically, the distance between the elements should be approximately $\lambda/4$ to $\lambda/6$ so that isolation can be minimized [7]. MIMO antennas are designed to have higher channel capacity and port isolation should be minimized so that higher port efficiency is achieved. Further, field correlation should be minimized, so channel paths are independent to have higher capacity.

In this step, second antenna is placed as 2×2 fashion with a distance between elements as 9.59 mm, horizontally and 5 mm vertically. MIMO 1, MIMO 2, MIMO3 and MIMO 4 are modified sequentially with ground plane to improve isolation, increase bandwidth and number of bands for operation. It is explained in further sections.

C. MIMO 1

Fig. 3 illustrates a structure of the MIMO1 antenna as front view (a) and back view (b). It has four ports, and they are excited with equal power. The back view shows ground in which SRR is added. It gives three bands having frequencies 3.69 GHz to 4.54 GHz, 4.86 GHz to 5.67 GHz, and 8.08 GHz to 8.45 GHz, respectively. Bandwidths measured at −10 dB are 855 MHz, 808.4 MHz, and 372.2 MHz, while impedance bandwidth (i.e., measured at −6 dB) is 3.12 GHz. Envelope correlation coefficient (ECC) is calculated from S-parameter and, it is well below 0.25. Diversity gain is also approaching 10 dB in a required band of operation.

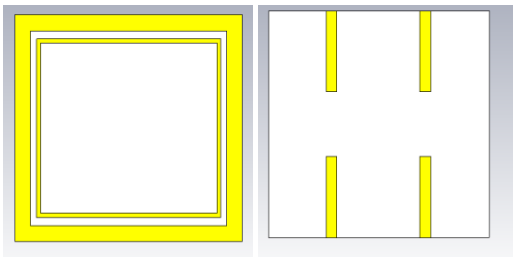

(a) (b)

Fig. 3. MIMO 1: (a) Front view and (b) back view.

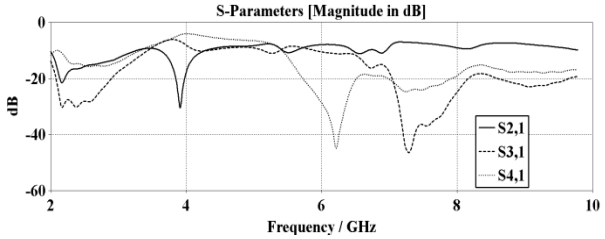

Fig. 4. Comparison of isolation between S21, S31, S41.

Isolation between Port 1-2 (S21), Port 1-3 (S31), and Port 1-4 (S41) are compared and shown in Fig. 4. It shows S21 as -30 dB at the first band and −11 dB for the second band. S31 and S41 are at −45 dB. S21 is not as per the required standard for the second band.

D. MIMO 2

Isolation S21 is more and because of which channel capacity loss is more. Therefore, as shown in Fig. 5 four square rings of 1 mm by 1 mm at 9.59 mm in horizontal and 5 mm in vertical with each other are added in ground structure. Because of modification in ground bandwidth is improved from 855 MHz to 1.89 GHz. Two bands are obtained as 3.51 GHz to 5.4 GHz and 7.9 GHz to 8.5 GHz. The bandwidths obtained are 1.89 GHz and 0.6324 GHz. Impedance bandwidth is 3.60 GHz and 3.21 GHz, respectively. Isolation between Port 1 and Port 2, S21 is −28 dB. Comparison between S21, S31, and S41 is shown in Fig. 5 (b), indicating S31 and S41 are well below −10 dB, but at a certain frequency it is more than 10 dB. Lower frequency bands are not obtained, so further changes are done.

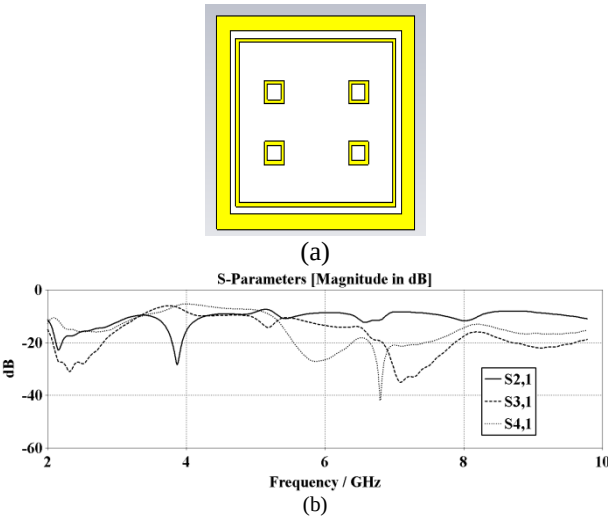

Fig. 5. MIMO 2 (a) back view of MIMO2 with modified DGS (b) Isolation comparison between Port 1, Port 2, Port 3, and Port 4.

E. MIMO 3

Fig. 6 shows the back view (a) of the MIMO3 antenna and isolation curve (b). The ground is further modified. More two slots are added in the ground so that square rings are connected horizontally. Because of the addition of slots in the ground multiple bands are obtained. Four bands are achieved as Band 1 (2.36-3.17) GHz, Band 2 (3.47-4.21) GHz, Band 3 (5.11-6.48) GHz, and Band 4 (7.88-9.01) GHz, respectively. Bandwidths are 810 MHz, 745 MHz, 1.367 GHz, and 1.13 GHz, respectively. The isolation curve is changed due to this modification as shown in Fig. 6 (b). Isolation S21 shows −15 dB for frequency from 4 GHz to 6 GHz. S31 shows −35 dB, −30 dB and −38 dB at resonating frequency. S41 shows isolation is below −15 dB for the required band of operation. Still, at some frequencies, isolation is not as per standard requirement, so further modification is done.

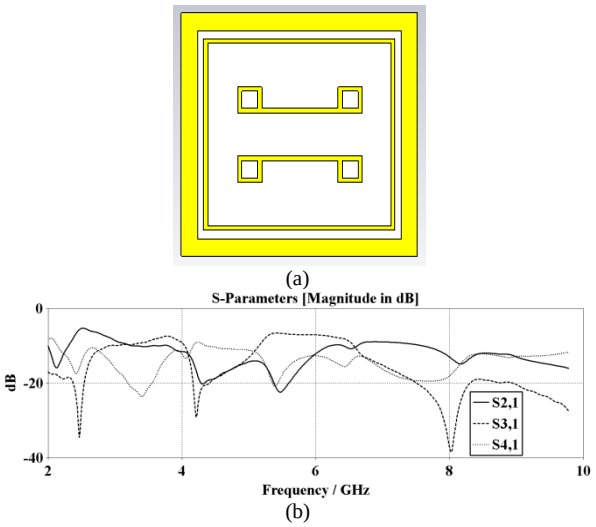

Fig. 6. MIMO 3 (a) back view of MIMO3 with modified DGS (b) Isolation comparison between Port 1, Port 2, Port 3, and Port 4.

F. MIMO 4

A further modification is done by adding two slots vertically so that square rings are added to each other, as shown in Fig. 7 (a).

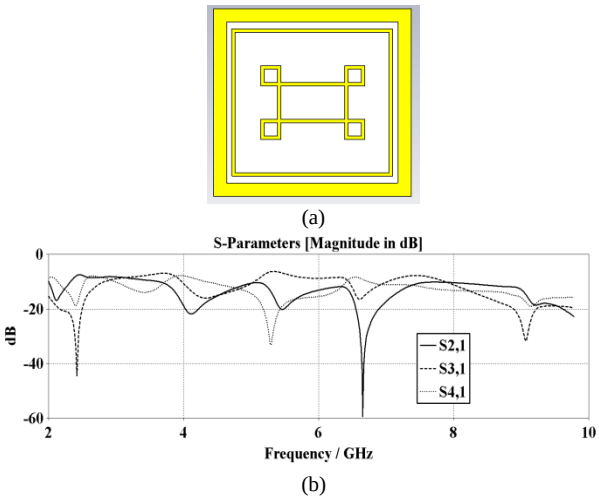

Fig. 7. MIMO 4 (a) back view of MIMO4 with modified DGS (b) Isolation comparison between Port 1, Port 2, Port 3 and Port 4.

Three bands obtained from this modification are Band 1 having frequency 2.42 GHz to 3.97 GHz, Band 2 5.12 GHz to 5.41 GHz, and Band 3 7.31 GHz to 9.25 GHz, respectively. Bandwidths are 1.55 GHz, 292 MHz, and 1.94 GHz, respectively. It shows improvement as compared to previous structures. Impedance bandwidth obtained is 8 GHz, this shows an ultra-wideband. The isolation plot as shown in Fig. 7 (b) indicates S21 is well below 10 dB. The lowest S21 is –60 dB.

Fig. 8 shows the radiation pattern in three dimensions for the structure. It gives a directivity of 5.46 dB. It also gives major and side lobes

Fig. 9 shows graph of maximum gain of MIMO4 antenna with respect to frequency. Maximum gain of 6.16 dB at frequency 8.19 GHz is measured. Efficiency in percentage is poltted against frequency as shown in Fig. 10. It indicates maximum efficiency of 62.96%.

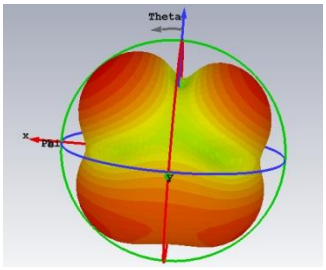

Fig. 8. The 3D radiation pattern for the MIMO4 antenna.

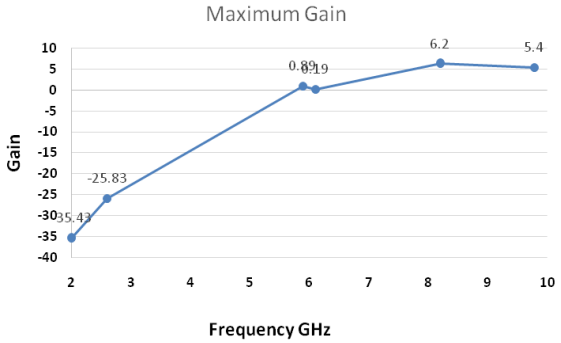

Fig. 9. Maximum gain over frequency curve.

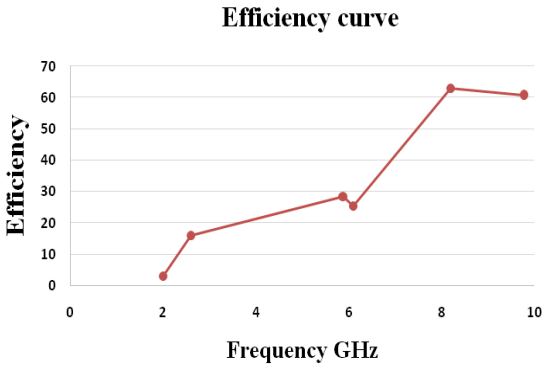

Fig.10. Total Efficiency in % over frequency.

III. Discussion

To verify the proposed structure for enhanced bandwidth and isolation, a prototype has been fabricated. Experimentation and detailed analysis of all performing parameters of MIMO antenna is provided in the following sub-sections.

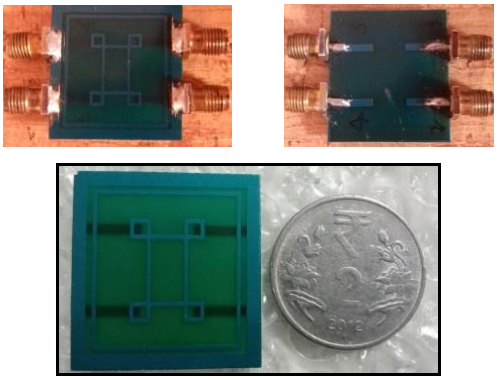

Fig. 11. Fabricated prototype of proposed MIMO antenna.

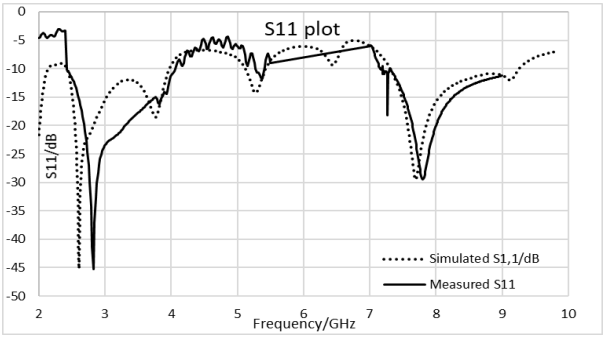

Fig. 12. Comparison of measured and simulated values of S11.

Fig. 11 shows fabricated prototype with connector as front view and back view. The size of the antenna is very compact as shown and compared with coin.

A. Scattering Parameters

Scattering(s) parameters are measured with the help of vector network analyzer Rohde & Schwarz ZVL (9 kHz to 13.8 GHz). S11 i.e., reflection coefficient for Port 1 is measured, while measuring S11, Port 2, Port 3, and Port 4 are terminated with a load impedance of 50 Ω.

Fig. 12 shows comparison of measured and simulated values of S11. It shows three bands. There is a slight frequency shift in measured value compared to simulated value as this happens due to material properties.

B. Isolation

Isolation becomes a more important parameter when the number of ports in a MIMO system increases. In literature, 10 dB isolation is considered as a reference. It means a minimum of 10 dB isolation is required between ports in the MIMO system. For four-port MIMO there exist mutual coupling terms S21, S31, and S41.

Fig. 13 shows comparison of measured and simulated values for S21, S31, and S41, respectively. It shows measured values are having better isolation as compared to simulated. Isolation enhancement is achieved in all the ports.

C. Surface Current

Surface current distribution for proposed MIMO antenna at 5.96 GHz frequency is measured at four ports. Magnitude of the current distribution of each port is shown in Fig. 14. When the ports are individually excited, better isolation is obtained among all ports of the antenna. Here negligible current flows amid the antenna elements when excited with other added ports.

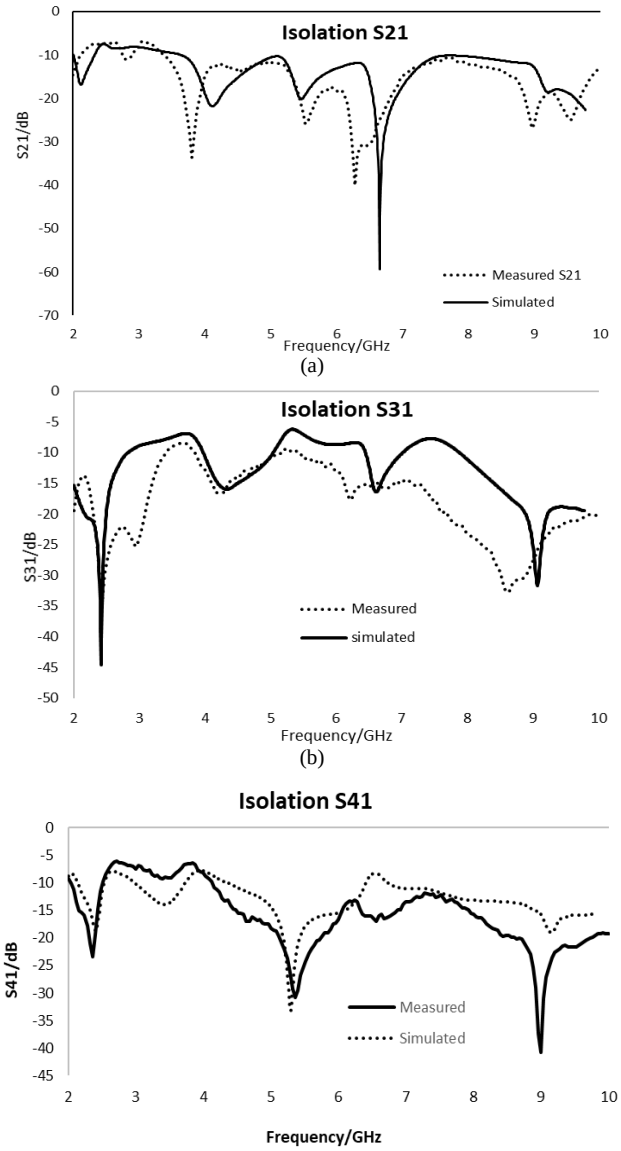

Fig. 13. Comparison of measured and simulated isolation between Port 1, Port 2, Port 3, and Port 4: (a) S21, (b) S31, and (c) S41.

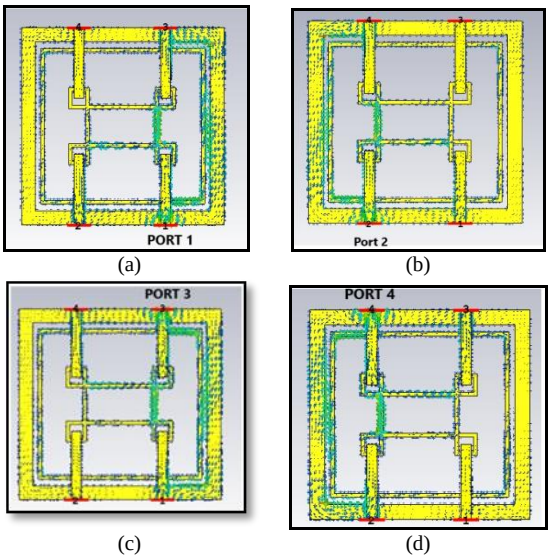

Fig. 14. Surface current distribution at 5.89 GHz at corresponding port excited (a) Port 1, (b) Port 2, (c) Port 3, and (d) Port 4.

D. Radiation Pattern

The radiation pattern of the proposed MIMO antenna has been evaluated. Two-dimensional (2D) radiation patterns of the MIMO Antenna 1, Antenna 2, Antenna 3, and Antenna 4 on the *x-z* plane at the frequency points of 5.89 GHz, are displayed in Fig. 15. Co and cross polarization are compared for all types of MIMO.

The radiation pattern of the proposed MIMO antenna is dumbbell-shaped in the E-plane and almost omnidirectional in the H-plane. As Antenna 1, Antenna 3, and Antenna 2, Antenna 4 are placed opposite to each other their pattern gets combined, and its bandwidth increases. Fig. 15 (a) and Fig. 15 (c) show co and cross-polarization for MIMO 1 and MIMO 3 antenna are the same. However, at higher frequencies, some deterioration is observed in the radiation pattern.

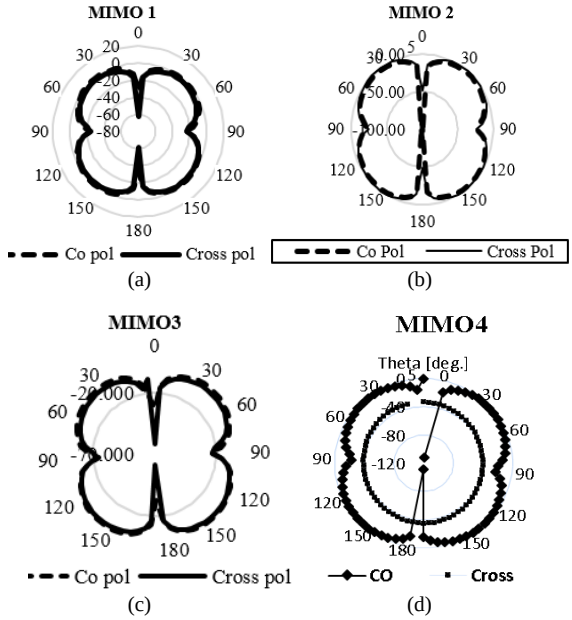

Fig. 15. Radiation Pattern of MIMO Antenna at 5.89 GHz (a) MIMO1 (b) MIMO2 (c) MIMO3 (d) MIMO4

E. Diversity Gain

The conditions for achieving good diversity gain are, the correlation coefficient between branch signals should be zero or "low" and mean Signal to Noise Ratio (SNRs) in each branch should be "similar". It can be calculated from S parameters as well as from far fields. The acceptable value of it should be 10 dB.

Fig. 16 shows diversity gain varies from 9.96 dB to 10 dB in a complete band of operation (2 GHz to 10 GHz). It has been taken from the S parameter.

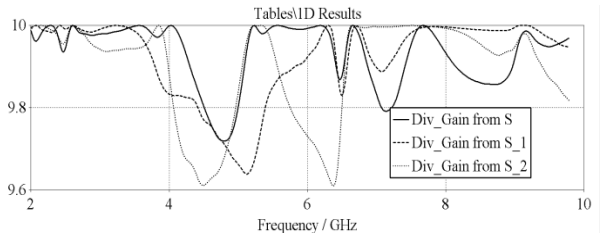

Fig. 16. Diversity Gain comparison between Port 1, Port 2, Port 3 and Port 4.

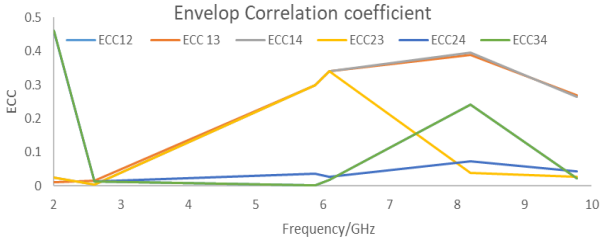

Fig. 17. ECC is measured from an electric field.

F. Envelop Correlation Coefficient

Calculating ECC between the two antenna elements gives an idea of how much the radiated signals from the two antenna elements are correlated with each other or diversified in space. The acceptable value of ECC is less than 0.5. ECC can be calculated either by using S-parameters or far-field patterns [8]. For high accuracy, ECC should be calculated from far-field pattern [10].

Fig. 17 shows an ECC graph which indicates the ECC value calculated from a far-field pattern and its value for the band of interest is 0.01. ECC12 is indicating a field correlation between Port 1 and Port 2. In similar ways, it has been taken as ECC13, ECC14, ECC23, ECC24, and ECC34. After comparing all these graphs, it has been concluded that the maximum value of ECC12 is 0.45 at a single frequency (8 GHz), for the rest of the band it is well below 0.1.

G. Testing with Software Defined Radio

The proposed MIMO antenna is also tested with SDR, as shown in Fig. 18. At the transmitter of SDR Port 1 of MIMO antenna is connected, Port 2 is terminated with 50-ohm impedance. Port 3 and Port 4 are connected to the power combiner circuit. It will take input from the array antenna, combine it, and give it to the receiver of SDR. With the help of a USB cable, it is connected to the laptop. With the help of software, parameters are verified. Data transmission and reception are also verified.

H. Comparison with References

The proposed MIMO antenna is compared with the existing MIMO antenna from the literature in Table II. It compares isolation enhancement techniques used, isolation, dimensions (compactness), number of elements, number of bands obtained, impedance bandwidth, and ECC. It is noted from Table II that with the proposed antenna achieves the highest impedance bandwidth: 2 GHz to 10 GHz and has compact size and three bands. ECC12 value varies with a band of operation. It is below 0.1 from 4 GHz to 6 GHz.

Fig.18. MIMO antenna with SDR.

TABLE II: COMPARISON OF MIMO ARRAY ANTENNA WITH LITERATURE

Reference	Isolation techniques	Isolation dB	Dimensions mm	No. of elements	Bands	Impedance Bandwidth GHz	ECC
[5]	Decoupling network	20	16×37.5×0.762	2	3-12	Not mentioned	<0.1
[7]	T shaped stub and CSRR	18	32×38×1.6	4	2-10	6.84	0.03
[23]	Microstrip transmission line with DRA	15	35×52.5×1.6	3	1-11	1.7-10.6	0.04
[8]	Un-protruded multi-slot	17.5	40×30×1.6	4	2-7	2.1	0.05
[9]	Triangular stub	19 at 2.4GHz 21 at 5.8GHz	89×86×1.6	4	2.4, 5.8	2.16–2.88 (0.72/29), 4.85–6.6 (1.75/31)	0.05
[10]	Chain shaped parasitic element	14	140×120	4	2.25-2.75	NM	<0.2
[25]	DRA	25	140×45×0.79	4	4.5-5.5	NM	0.2
[20]	Fractal MTM-EMBG	17	90×120×1.6	4	NA	1.25 for 8 to 9.25	0.02
Proposed	SRR and slots	45 at 2.4 and 9 GHz	28×29.58×0.8	4	2.42-3.97, 5.12-5.41, 7.31-9.25	8	0.1

IV. CONCLUSION

A compact microstrip MIMO array antenna for wireless PAN application is proposed in this paper. The MIMO configuration is simulated, fabricated, and tested. The square ring resonator and slots show enhanced bandwidth (from 3.12 GHz to 8 GHz) with three bands. The antenna elements 1, 3, and 2, 4 are orthogonally placed, which results in pattern diversity of the MIMO antenna. MIMO antenna also shows good diversity performance in terms of ECC (0.01) and diversity gain (10 dB). All simulated results show great concurrence with the measured results. The omnidirectional radiation pattern of the antenna makes it suitable for wireless application.

CONFLICT OF INTEREST

The authors declare no conflict of interest.

AUTHOR CONTRIBUTIONS

Shilpa Nandedkar conducted the research and wrote the paper and Shankar Nawale reviewed and approved the final version.

REFERENCES

[1] F. Flaviis, L. Jofre, J. Romeu, and A. Grau, *Multi-Antenna Systems for MIMO Communications*, Morgon & Claypool, 2008, pp. 7-10.

[2] S. Li, J. Gao, Y. Zhao, Z. Zhang, and H. Liu. "Loading meta material perfect absorber method for in-band radar cross-section

reduction based on the surface current distribution of array antennas," *IET Microw. Antennas Propag*, vol. 9, no. 5, pp. 399–406, 2015.
[3] R. Sahoo and D. Vakula, "Gain enhancement of conformal wideband antenna with parasitic elements and low index metamaterial for WiMAX application," *AEU - International Journal of Electronics and Communications*, vol. 105, pp. 24–35, June 2019.
[4] S. Zhang and G. F. Pedersen, "Mutual coupling reduction for UWB MIMO antennas with a wideband neutralization line," *IEEE Antennas Wirel. Propag. Lett.*, vol. 15, pp. 166–169, 2016.
[5] D. Sipal, M. Abegaonkar, and S. Koul, "UWB MIMO USB dongle antenna for the personal area network application," in *Proc. of APMC Conf. Asia-Pacific Microwave*, 2017, pp. 8–11.
[6] N. Chalok, M. Yilmaz, H. Arslan, and M. Ali, "High-gain pattern reconfigurable MIMO antenna array for wireless handheld terminals," *IEEE Trans. on Antennas Propagation*, vol. 64, no. 10, pp. 4306–15, Oct. 2016.
[7] S. Kumar, R. Kumar, V. Kumar, and K. Srivastava, "An improved compact MIMO antenna for wireless applications with band-notched characteristics," *AEU - International Journal of Electronics and Communications*, vol. 90, pp. 20–29, June 2018.
[8] J. Kulkarni, A. Desai, and C. Sim, "Wideband four-port MIMO antenna array with high isolation for future wireless systems," *AEU - International Journal of Electronics and Communications*, vol. 128, Jan. 2021.
[9] A. Birwal, S. Singh, B. Kanaujia, and S. Kumar, "Low-profile 2.4/5.8 GHz MIMO/diversity antenna for WLAN applications," *Journal of Electromagnetic Waves and Applications*, vol. 34, no. 9, pp. 1283–1299, 2020.
[10] A. Moradi, R. Ngah, and M. Khalily, "Polarized diversity compact planar MIMO antenna for wireless access point applications," *Progress in Electromagnetics Research C*, vol. 91, pp. 115–127, Mar. 2019.
[11] J. Malik, D. Nagpal, and M. Kartikeyan, "MIMO antenna with omnidirectional pattern diversity," *Electronics Letter*, vol. 52, no. 2, pp. 102–104, January 2016.
[12] S. Mikki, S. Clauzier, and Y. Antar, "Empirical geometrical bounds on MIMO antenna arrays for optimum diversity gain performance, An electromagnetic design approach," *IEEE Access*, vol. 6, pp. 39876–94, Aug. 2018.
[13] K. Zhi, C. Pan, H. Ren, and K. Wang, "Statistical CSI-based design for reconfigurable intelligent surface-aided massive MIMO systems with direct links," *IEEE Wireless Communication Letter*, 2021.
[14] W. Tang, J. Dai, M. Chen, K. Wong, X. Li, and X. Zhao, "MIMO transmission through reconfigurable intelligent surface: system design, analysis, and implementation," *IEEE Journal on Selected Areas in Communications*, vol. 38, no.11, pp. 2683–2699, July 2020.
[15] L. You, J. Xiong, Y. Huang, D. Ng, C. Pan, and W. Wang, "Reconfigurable intelligent surfaces-assisted multiuser MIMO uplink transmission with partial CSI," *IEEE Trans. Wireless Communications*, vol. 20, no. 9, pp. 5613-5627, 2021.
[16] N. Parchin, H. Basherlou, A. Yasir, *et al.*, "Recent developments of reconfigurable antennas for current and future wireless communication systems," *Electronics*, vol. 8, no. 2, 2019.
[17] J. M. Hannula, J. Holopainen, and V. Viikari, "Concept for frequency-reconfigurable antenna based on distributed transceivers," *IEEE Antennas and Wireless Propagation Letters*, vol. 16, pp. 764–767, 2017.
[18] V. N. K. R. Devana and A. M. Rao, "Compact 3.1- 18.8 GHz triple band notched UWB antenna for mobile UWB applications," *IRO Journal on Sustainable Wireless Systems*, vol. 2, pp. 1–12, Mar. 2020.
[19] L. Liu, S. Cheung, and T. Yuk, "Compact MIMO antenna for portable UWB applications with band-notched characteristic," *IEEE Trans on Antennas and Propagation*, vol. 63, no. 6, pp. 1917–1924, 2015.
[20] M. Alibakhshikenari, B. Virdee, C. See, R. Alhameed, A. H. Ali, and F. Falcone, "Study on isolation improvement between closely-packed patch antenna arrays based on fractal metamaterial electromagnetic bandgap structures," *IET Microwaves, Antennas and Propagation*, vol. 12, pp. 2241–2247, Oct. 2018.
[21] P. Das, A. K. Singh, and K. Mandal, "Metamaterial loaded highly isolated tunable polarisation diversity MIMO antennas for THz applications," *Optical and Quantum Electronics*, vol. 54, no. 4, pp. 1–19, March 2022.
[22] G. Das, A. Sharma, R. Gangwar, and M. Sharawi, "Compact back-to-back DRA-based four-port MIMO antenna system with bi-directional diversity," *Electronics Letters*, vol. 54, no. 14, pp. 884–886, July 2018.
[23] S. Pahadsingh and S. Sahu, "Four-port MIMO integrated antenna system with DRA for cognitive radio platforms," *AEU - International Journal of Electronics and Communications*, vol. 92, pp. 98–110, Aug. 2018.
[24] M. Sharawi, S. Podilchak, M. Khan, and Y. Antar, "Dual-frequency DRA-based MIMO antenna system for wireless access points," *IET Microwaves, Antennas Propagation*, vol. 11, pp. 1174–1182, May 2017.
[25] G. Sarkar, S. Balav, A. Chatterje, S. Ranjit, and S. Parui, "Four element MIMO DRA with high isolation for WLAN applications," *Progress in Electromagnetics Research Letters*, vol. 84, pp. 99–106, May 2019.
[26] Q. Luo, J. R. Pereira, and H. Salgado, "Low-Cost compact multiband printed monopole antennas and arrays for wireless communications," in *Progress in Compact Antennas*, L. Huitema Ed., 2014.

Shilpa Nandedkar is presently an Assistant Professor in the Electronics and Telecommunication Engineering Department at Maharashtra Institute of Technology, Aurangabad. She completed B.E. and M.E. in Electronics and Telecommunication Engineering from Dr. Babasaheb Ambedkar Marathwada University, Aurangabad. She is a Doctoral Scholar at Dr. Babasaheb Ambedkar Marathwada University in the Department of Electronics and Telecommunication. Her interests are in UWB antenna, MIMO systems, and Wireless Networks. She is a Graduate student member of IEEE. She received the best paper award at the IEEE conference.

Shankar Nawale has received M. Tech. and Ph.D. degrees in electronics & telecommunication engineering from Mumbai University, India in 2008 and 2013 respectively. He carried out post-doctoral research in LCIS Lab at Grenoble Institute of Technology (Grenoble INP), Valence, France 2014. His research lies in the area of passive RFID tags and its applications for environmental monitoring and electromagnetic energy harvesting. He has total twenty-one years of experience which includes teaching, research and administration. He has been a teacher in the subjects of Electromagnetics, Antennas, Wave Propagation, Microwave Engineering, Wireless and Mobile Communication during his career as a Lecturer, Assistant Professor, Associate Professor and a Professor. Shankar has thirty-five publications in Peer Reviewed Journals and reputed conferences. He is a co-author of two books on RFID passive tags. He is also a reviewer of journals of IEEE, Springer, Wiley and Cambridge press. Shankar has visited almost 10 countries for research, conference or symposium purpose. Currently Shankar is working as a Principal of NBN Sinhgad College of Engineering, Solapur and Dean, Faculty of Science & Technology, PAH Solapur University Solapur, India.